ARTICLE OPEN ACCESS

Baicalin Promotes CNS Remyelination via PPARγ Signal Pathway

Ruo-Song Ai, PhD,* Kun Xing, MSc,* Xin Deng, MSc,* Juan-Juan Han, MSc,* Dong-Xia Hao, MSc, Wen-Hui Qi, MSc, Bing Han, PhD, Ya-Na Yang, MSc, Xing Li, PhD, and Yuan Zhang, PhD

Correspondence
Dr. Zhang
yuanzhang_bio@126.com

Neurol Neuroimmunol Neuroinflamm 2022;9:e1142. doi:10.1212/NXI.0000000000001142

Abstract

Background and Objectives

Demyelinating diseases in the CNS are characterized by myelin sheath destruction or formation disorder that leads to severe neurologic dysfunction. Remission of such diseases is largely dependent on the differentiation of oligodendrocytes precursor cells (OPCs) into mature myelin-forming OLGs at the demyelinated lesions, which is defined as remyelination. We discover that baicalin (BA), a natural flavonoid, in addition to its well-known antiinflammatory effects, directly stimulates OLG maturation and CNS myelin repair.

Methods

To investigate the function of BA on CNS remyelination, we develop the complementary in vivo and in vitro models, including physiologic neonatal mouse CNS myelinogenesis model, pathologic cuprizone-induced (CPZ-induced) toxic demyelination model, and postnatal OLG maturation assay. Furthermore, molecular docking, pharmacologic regulation, and transgenic heterozygous mice were used to clarify the target and action of the mechanism of BA on myelin repair promotion.

Results

Administration of BA was not only merely effectively enhanced CNS myelinogenesis during postnatal development but also promoted remyelination and reversed the coordination movement disorder in the CPZ-induced toxic demyelination model. Of note, myelin-promoting effects of BA on myelination or regeneration is peroxisome proliferator-activated receptor γ (PPARγ) signaling-dependent.

Discussion

Our work demonstrated that BA promotes myelin production and regeneration by activating the PPARγ signal pathway and also confirmed that BA is an effective natural product for the treatment of demyelinating diseases.

*Equal Contributions to this work and are the co–first authors of this paper.

From the Shaanxi Normal University, Xi'an, China.

Go to Neurology.org/NN for full disclosures. Funding information is provided at the end of the article.

The Article Processing Charge was funded by the authors.

Glossary

APC = adenomatous polyposis coli; **BA** = baicalin; **CGZ** = ciglitazone; **CPZ** = cuprizone; **EAE** = experimental autoimmune encephalomyelitis; **GFAP** = glial fibrillary acidic protein; **IBA1** = ionized calcium binding adapter molecule 1; **LFB** = Luxol fast blue; **MBP** = myelin basic protein; **MS** = multiple sclerosis; **NC** = naïve chow; **NFH** = neurofilament H; **NG2** = chondroitin sulfate proteoglycan 2; **OLGs** = oligodendrocytes; **Olig2** = oligodendrocyte transcription factor 2; **OPCs** = oligodendrocyte precursor cells; **PBS** = phosphate-buffered saline; **PDGFR α** = platelet-derived growth factor receptor α; **PEI** = polysciences; **PGZ** = pioglitazone; **PPARγ** = peroxisome proliferator-activated receptor γ; **PPARγ$^{+/-}$** = PPARγ deficient heterozygous; **PPRE** = peroxisome proliferator element.

Demyelinating lesions and axonal damage are common pathologic characteristics of various CNS diseases such as multiple sclerosis (MS), leukodystrophy, stroke, spinal cord injury, Alzheimer disease, Parkinson disease, chronic hypoxia, and cerebral small vessel disease.[1-3] Failure of remyelination is an important pathogenesis and therapeutic target of white matter demyelinating diseases.[4,5] Demyelination in the CNS is usually a consequence of a direct insult of the oligodendrocytes (OLGs), the CNS myelin-forming cells originating from the development of oligodendrocyte precursor cells (OPCs).[4] During the spontaneous myelinogenesis, OPCs develop into mature OLGs to achieve myelination by activation, migration recruitment, proliferation, and differentiation.[4,5] Several researchers have reported that the accumulation of OPCs is frequently observed in demyelinated lesions of patients with MS,[6] but these cells rarely mature into OLGs. A previous study has shown that during the disease progression of animal model of MS, accompanying with the significant myelin loss, OPCs clustered at the demyelinating lesions in the CNS, whereas they did not differentiate normally. These data suggested that the ability of activation, migration, or proliferation of OPCs to the demyelinated lesion is sufficient for remyelination, and the major limitation impeding the repair of injured myelin sheath is the failure of OPC differentiation.[7] Therefore, pharmacologic regulation of remyelination by targeting OPC differentiation is a promising strategy for the treatment of demyelinating neurologic diseases.

Natural products are a rich resource for discovering effective candidate drugs in clinical application. Baicalin (BA), a flavonoid compound (molecular weight 446.37) isolated from the root of medicinal plant *Scutellaria baicalensis* Georgi, has been used for the treatment of a variety of acute and chronic hepatitis in clinic.[6,8] It is reported that BA is a safe and effective drug with significant biological activities, such as anti-inflammatory, antibacterial, anticancer, and promoting hippocampal neurogenesis, and it has been applied in animal models of arthritis, Alzheimer disease, and MS.[6,9] Our previous study demonstrated that oral BA effectively ameliorated clinical disease severity of experimental autoimmune encephalomyelitis (EAE), an animal model of MS, and reduced the inflammation and demyelination of the CNS,[10] indicating its potential application on demyelinating disease. However, the efficacy of BA for inhibiting demyelination might be the secondary effects of its well-known anti-inflammatory activity. Whether BA functions on OPC differentiation and remyelination directly is hardly known.

In this study, the authors sought to investigate the role of BA on myelination and/or remyelination based on myelinogenesis and cuprizone (CPZ)-induced demyelination animal model, as well as its direct function on the development of primary OPCs in vitro. Notably, the administration of BA was not only merely effectively enhanced CNS myelinogenesis during postnatal development but also promoted remyelination and reversed the coordination movement disorder in the CPZ-induced demyelination model. Furthermore, the action of the mechanism of BA on myelin promotion depended on its direct interaction with peroxisome proliferator-activated receptor γ (PPARγ).

Methods

Standard Animal Protocol Approvals and Registrations

All animal experimental procedures and protocols using mice were approved by the Committee on the Ethics of Animal Experiments of Shaanxi Normal University (No. SCXK-2018-001) and were carried out in accordance with the approved institutional guidelines and regulations. The mice were fed under standard light and temperature conditions and provided with free access to water and food.

CNS Myelinogenesis Model

C57BL/6 mice, 3–21 days after birth, purchased from the Animal Experiment Center of Air Force Military Medical University (Xi'an, China). Because some variability was observed among different mouse litter, littermates of similar weight were paired and assigned to the litter in all experiments performed. The stock solution of BA (Sigma-Aldrich, St. Louis, MO) was prepared in DMSO (1 mg/mL). BA treatment was applied by consecutive 12 daily subcutaneous injections, 100 mg/kg/d according to our previous optimal results,[10] starting at postnatal days 3–14. Littermate mice were treated by phosphate-buffered saline (PBS) as sham control. Mice were euthanized and perfused with PBS. The brain and the lumbar enlargement of the spinal cord were dissected and postfixed in paraformaldehyde (4% for 24 hours and then 30% sucrose solution in PBS for 48 hours, in 4°C)

and then tissues were removed for histopathologic, immunohistochemistry, and electron microscopy analyses.

CPZ-Induced Demyelination Model

C57BL/6 male mice (8–10 weeks of age) and PPARγ$^{\pm}$ mice (C57BL/6J background) were purchased from The Jackson Laboratory (Bar Harbor, ME) and were used in the CPZ-induced model. Mice were fed with 0.2% CPZ (Sigma) mixed into a ground standard rodent chow. Cuprizone diet was maintained for 6 weeks to induce demyelination. Thereafter, cuprizone chow was removed, and the mice were given normal chow to check myelin sheath spontaneous recovery efficiency. The mice receive daily intraperitoneal injection of BA (100 mg/kg/d) or PBS until 6 + 3 weeks. Mice were euthanized and corpus callosum of brain tissue was collected and placed in RNA storage solution (in 4°C overnight, −80°C store) for subsequent RNA extraction. For histology, all mice were anesthetized and perfused with PBS, and the brain was dissected and postfixed in paraformaldehyde (4% for 24 hours and then 30% sucrose solution in PBS for 48 hours, in 4°C) and then sectioned and stained for histopathologic analysis.

Primary OPC Cultures

Primary OPCs were isolated according to our previous study.[11] Briefly, brains of C57BL/6 mice pups (postnatal days 0–7, mixed sex) were quickly harvested on ice-cold HBSS. After the removal of the meninges and blood vessels, brains were triturated and then dissociated with Neural Tissue Dissociation Kit (Miltenyi Biotech Inc.) at 37°C. Cells were subsequently sorted with CD140a (PDGFRα) MicroBead Kit on ice (Miltenyi Biotech Inc). Afterward, the cells were plated on poly-D-lysine and laminin-coated dishes and cultured in DMEM/F12 supplemented with 2% B27, 1% N2, 2 mM GlutaMAX, 20 ng/mL PDGF-AA, and 20 ng/mL bFGF. For differentiation, the proliferation medium for OPCs was replaced by DMEM/F12 with 2% B27, 1% N2, 30 ng/mL T3, 50 ng/mL, and 50 ng/mL noggin and changed every 2 days. OPCs were also treated with the PPARγ inhibitor GW9662 (1 μM) or vehicle for 30 minutes, followed by coincubation with BA (1, 5, or 10 μg/mL) or vehicle for 5 days. Immunostaining of mature OL marker myelin basic protein (MBP) was performed 5 days after treatment.

Molecular Docking

The molecular docking map of BA into the PPARγ active pocket was obtained by using the molecular docking technique, which showed that BA had hydrogen bond interactions with the protein structure of PPARγ at multiple positions (AutoDock Vina software, virtually screened model: PDB-2Q55). Subsequently, MST affinity assay experiments were performed, and the results showed that the dissociation constant of BA and PPARγ was 1.35 μM, indicating that the 2 had affinity cooperation, which was consistent with the results of molecular docking.

Transient Transfection and Luciferase Reporter Assay

The plasmid pCDH-CMV-MCS-EF1α-copGFP (System-Biosciences, California) was used as a backbone, and the PPARγ sequence was inserted to the Mcs site to generate a PPARγ overexpression lentivirus vector (mPPARγ-OE). HEK293T cells transfected with lentiviral mPPARγ-OE were plated in 96-well plates at a density of 2×10^5 per well, 100 μL/well, and cultured in a cell constant temperature incubator at 37°C and 5% CO_2. After overnight cell culture, plasmid transfection was performed. Peroxisome proliferator element (PPRE) ×3-TK-luciferase plasmid and polysciences (PEI) were added into the DMEM, respectively, mixed well, and allowed to stand at room temperature for 5 minutes; then, the DMEM containing the plasmid was added into the DMEM-containing PEI, mixed well, and placed at room temperature for 20 minutes and later added into the corresponding well. Complete DMEM (DMEM-high glucose containing 10% FBS, 1% penicillin-streptomycin) was replaced after 6 hours. After 18 hours of transfection, cells were stimulated with different concentrations of BA. PPRE-luciferase reporter assay, Renilla luciferase, was monitored in cell lysates by using Dual-Glo Luciferase Assay kit (Promega) according to the manufacturer's instructions.

Behavioral Assessments

Sensorimotor and coordination ability were assessed by investigators blinded to group assignments. Behavior tests were performed according to the described method below at a specific time point. After each test, the instrument was cleaned with 75% alcohol to prevent affecting the results of the next mouse.

Beam walking: the balance beam was 1 m long and 10 mm wide, which was 60 cm from the ground, and one end was suspended, whereas the other end served as an escape platform with a mouse cage and the chow. During the experiment, the mice were placed at the suspended end of the balance beam, and the time to reach the escape platform was recorded for each experimental mouse (the maximum monitoring time was 60 seconds, and if the escape platform was not reached, it was recorded as 60 seconds), and 3 experiments were performed for each mouse, with an interval of 60 seconds between each experiment. The final results were averaged over the 2 latter times.

Wire hang test: the 2 ends of a 2-mm diameter rope were tightened on two 60 cm tall platforms separated by 50 cm to prevent mice from falling; sponge pads were placed below the rope. For the experiment, the mouse was placed in the right middle of the tightrope, and the time the mouse reached the platform at either end from the middle of the tightrope was recorded (the maximum monitoring time was 60 seconds, and if the escape platform was not reached, it was recorded as 60 seconds). Three trials were performed for each mouse, with an interval of 60 seconds between each experiment. The ultimate results were averaged over the last 2 times.

Before the start of the experiment, mice learned to maintain balance and movement on a fatigued rotarod instrument and adapted for 5 minutes at 5 rpm. For the experiment, the mice were placed on the rotarod instrument at an initial speed of 5 rpm, which was accelerated at a rate of 1 rpm per s until the mice fell, and the latency to fall was recorded. Two experiments were performed for each mouse with a 60-second interval between the 2 experiments, and the ultimate results were averaged over 2 times.

Real-Time RT-PCR

Total RNA was isolated from brain tissues using RNAprep Pure Tissue Kit (TIANGEN BIOTECH, Beijing, China) according to the manufacturer's instructions. Reverse transcription was conducted by using PrimeScript RT Master Mix Kit (TaKaRa Biotechnology, Dalian, China). RT-PCR was performed by LightCycler 96 System (Roche) and ChamQTM Sybr qPCR Master Mix (Vazyme Biotech, Nanjing, China) was used for the reaction. GAPDH was used as an internal normalized control. RT-PCR primers for mouse gene sequences were listed in eTable1, links.lww.com/NXI/A691.

Histology and Immunofluorescent Analysis

Mice were deeply anesthetized and perfused transcardially. Corpus callosum was cut into thin sections of 1 mm^3 in sterile petri dishes and then postfixed in TEM fixative (Seville Biotechnology Co. LTD, China) at room temperature, for 60 minutes, and transfered to 4°C for 24 hours. Tissues were washed 3 times with PBS, postfixed in 1% osmium tetroxide in PBS for 2 hours at room temperature, washed 3 times with PBS, 15 minutes each, and dehydrated in graded ethanol solutions. Subsequently, the samples was embedded in Epon-Araldite resin for penetration and placed in a mold for polymerization. The tissues were polymerizated, and ultrathin sections (60–80 nm) were obtained using UC7 (Leica). Tissues were fished out onto the 150 meshes cuprum grids with formvar film. Staining was performed with 2% uranium acetate saturated alcohol solution and examined by using light microscopy (HT7800, Hitachi) for histologic assessment, and photographs were obtained. Images were analyzed in Image-Pro for the thickness of myelin sheath and g-ratio.

Paraffin-embedded coronal sections of the brains were stained with Luxol fast blue (LFB) for analysis of demyelination. Images were taken, and a quantitative image analysis was performed using Image-Pro software.

For immunohistochemistry, the thorax spinal cord segments and brain segments were OCT compound (Tissue-tek, Sakura Finetek, Japan) embedded and sectioned coronally (6–8 μm) by freezing microtome (Leica, Nussloch, DE). The frozen section was returned to room temperature and fixed in acetone for 3 minutes. The slices were then washed 3 times with PBS and permeabilizated and preincubated in a blocking buffer for 60 minutes, and then incubated overnight with primary antibodies at 4°C. The following antibodies were used: rabbit anti-OLG transcription factor 2 (Olig2, Abcam, Cambridge, UK), rabbit antichondroitin sulfate proteoglycan 2 (NG2, Abcam), mouse antiadenomatous polyposis coli (APC, clone CC-1, Calbiochem), rabbit antimyelin basic protein (MBP, Abcam), chicken antineurofilament H (NFH, Millipore, MA), mouse antiglial fibrillary acidic protein (GFAP, Millipore), and rabbit-ionized calcium binding adapter molecule 1 (IBA1, WAKO, Tokyo, Japan). After thorough washing, the sections were stained with secondary antibody conjugated to Alexa Fluor 488 or Alexa Fluor 594 (Jackson ImmunoResearch Laboratories, Inc), and nuclei were stained with DAPI. FluoroMyelin was conducted by BrainStain Imaging Kit (Invitrogen, Grand Island, NY). Images were taken using a Nikon Eclipse E600 inverted fluorescent microscope, and a quantitative image analysis was performed using Image-Pro and ImageJ.

For immunocytochemical staining, OPCs were fixed with 4% paraformaldehyde for 30 minutes at room temperature and washed 3 times with PBS. Coverslips with cells were permeabilized with 0.3% Triton X-100 for 15 minutes at room temperature and were preincubated in PBS solution containing 10% normal horse serum for 60 minutes, and then incubated overnight with primary antibodies at 4°C. After thorough washing, the sections were stained with secondary antibody conjugated to Alexa Fluor 488 or Alexa Fluor 594 (Jackson ImmunoResearch), and nucleus was stained with DAPI. Slides were covered with mounting medium (Vector Laboratories, Burlingame, CA). Images were taken using a Nikon Eclipse E600 inverted fluorescent microscope, and a quantitative image analysis was performed using Image-Pro or ImageJ.

Statistical Analysis

All statistical analyzes were performed by using GraphPad Prism 8.0 software (GraphPad software, La Jolla, CA). The results are described as mean ± SEM. Statistical difference groups were implemented by an analysis of 2-tailed Student *t*-test and analysis of variance with Tukey multiple comparisons test. $p < 0.05$ was considered statistically significant. Statistical details are given in the figure legends.

Data Availability

The data set used and analyzed during this study is included in the main text, or the supplementary files, or is available from the corresponding author on reasonable request.

Results

BA Enhances CNS Myelinogenesis During Postnatal Development

Previous studies have demonstrated that the intensive myelination of C57BL/6 mice occurs postnatally during the first 3 weeks of their life, when the myelin sheath develops significantly. To understand whether BA influenced myelination during postnatal development, we first detected the expression of specific proteins at different stages of OLG maturation and then investigated its effect on the OPC differentiation in the CNS (Figure 1A). To find out the effect of BA on the

Figure 1 BA Enhances CNS Myelinogenesis During Postnatal Development

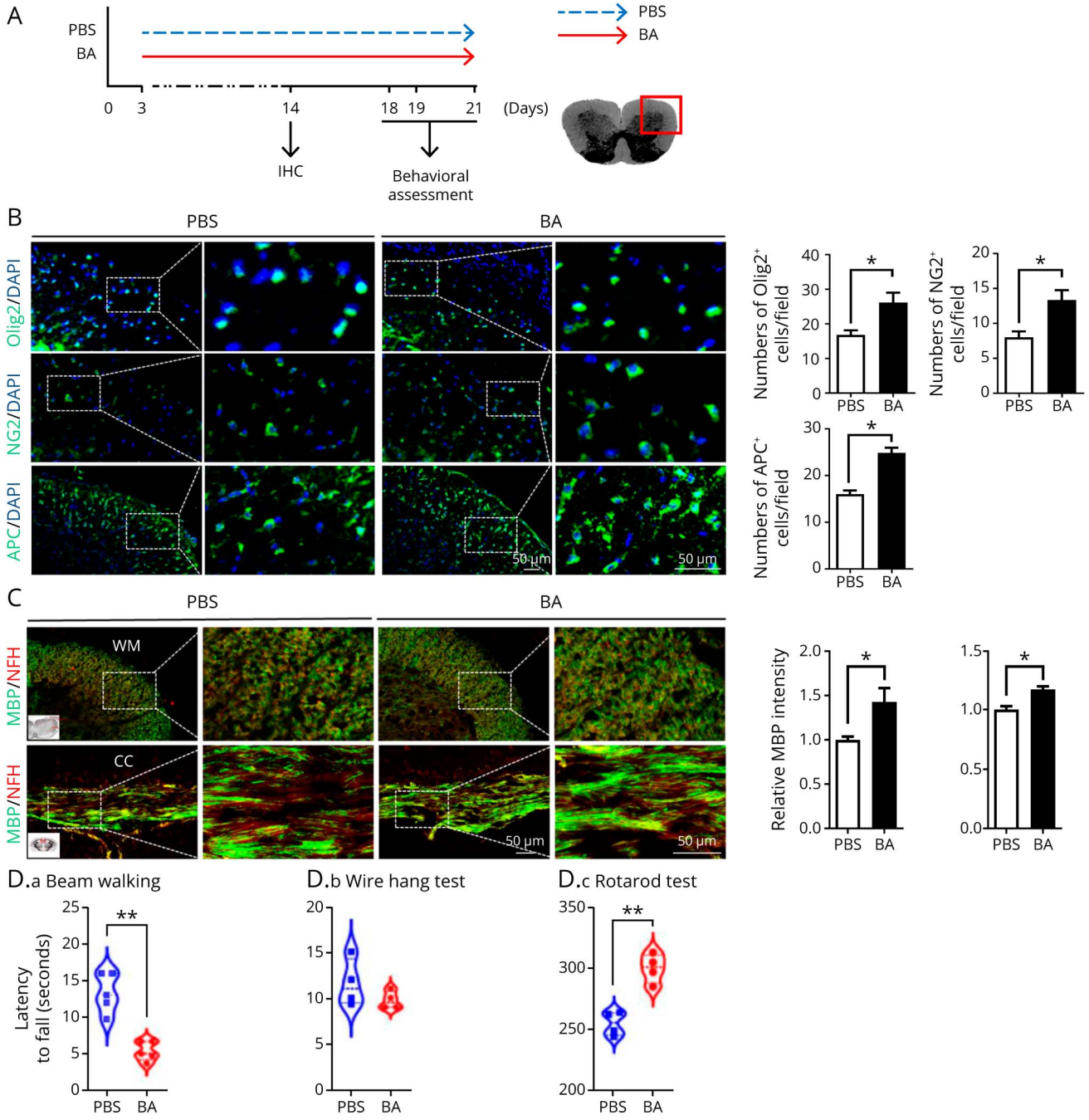

(A) Treatment paradigms. (B) Representative sections stained for Olig2, NG2, APC, and DAPI of spinal cord segment harvested on postnatal day 14 (Scale bar = 50 μm). Quantifications were performed by counting the Olig2, NG2, and APC positive nucleated cells at random areas. (C) Ventral roots of peripheral motor nerve at the level of the lumbar spinal cord segment and corpus callosum harvested on postnatal day 14 were stained for myelin with antibodies to MBP and for axonal fibers with antibodies for neurofilament H (Scale bar, 50 μm). MBP intensity was measured in the ventral roots of spinal cord or corpus callosum using Image-Pro. (D.a-c) D.a: Beam walking test was performed on postnatal day 18, and the latency to traverse each beam and the time the hind feet slip off each beam are recorded for each trial. D.b: The wire hang test was performed on postnatal day 19. Mice received 2 consecutive trials, and the latency to traverse the beam was recorded for each trial (cutoff time 60 seconds). D.c: The rotarod test was performed on postnatal day 21, and the latency to fall off the rod and the actual rotating speed level was measured. The average latency of falling off the rod and the average actual rotating speed was recorded. Data of (B, C, D) are shown as mean values ±SEM and analyzed by 2-tailed Student *t*-test (n = 5 each group). *$p < 0.05$, **$p < 0.01$, and ***$p < 0.001$. BA = baicalin.

OLG lineage cell, we used this marker, Olig2, which is more expressed to this lineage. The number of Olig2$^+$ cells in the white matter of BA-treated mice was higher than those of PBS-treated infant mice, being consistent with the constitutive expression of Olig2 on subsequent maturation stages (Figure 1B, $p < 0.05$). As shown in Figure 1B, NG2 (OPC marker at early development stage)-positive cells were present in the white matter of the spinal cords of the PBS-treated infant mice, the number of which is 1.5-fold lower than that of BA-treated group. To identify the effects of BA treatment on

mature OLGs, spinal cord sections were stained by APC, a marker of mature oligodendroglia. A quantitative analysis of APC-expressing cells at postnatal day 14 showed that in the BA-treated group, the number of APC^+ OLGs were significantly higher than those in PBS-treated control (Figure 1B, $p < 0.05$). These findings indicated the promotion of OPC differentiation and maturation in the CNS of BA-treated mice.

We then investigated the effects of BA on CNS myelinogenesis during postnatal development by using anti-MBP (myelin marker) and anti-NFH (NFH; axonal marker) staining. As shown in Figure 1C, mice treated with BA had a significantly higher intensity of MBP expression and greater number of myelinated axons (MBP^+ NFH^+) compared with the PBS-treated control.

The development of myelin sheath is closely related to animal motor coordination.[12,13] To investigate whether BA-induced myelin development affects motor function, we performed behavioral assessment of mice treated by BA or PBS at postnatal days 18–21. The time of BA-treated mice traverse faster on a narrow beam than that of PBS-treated control mice in the beam walking assay (Figure 1D, $p < 0.01$), whereas the 2 groups show similar activity of locomotor and directed exploration in the wire hang test ($p > 0.01$). In the rotarod test, the latency to fall of BA-treated mice was increased remarkably than that of the control ($p < 0.01$). These results indicated that the enhanced CNS myelination and movement coordination ability of newborn mice were induced by BA because of its promotion effects on OLG differentiation.

BA Enhances Remyelination in CPZ-Induced Demyelination

To further investigate the direct effects of BA on remyelination in vivo, we used the toxic CPZ-induced demyelination model. This model is widely accepted for studying the effects of drugs on demyelination and remyelination processes in the CNS. In contrast to the immune-induced demyelination animal model-like EAE, the blood–brain barrier of CPZ-induced mice occurs intact, which allows us to analyze the pathomechanisms of remyelination bypassing possible interference of peripheral immune cells.

Mice were fed with CPZ-containing chow for 6 weeks to achieve complete demyelination in the corpus callosum. CPZ was then withdrawn, and mice were fed with normal chow, allowing for spontaneous remyelination to take place within the next 2 weeks. Mice were administrated with either BA (100 mg/kg/d) or PBS along with CPZ-containing chow beginning at 0 weeks and continuing treatment until 6 + 3 weeks (Figure 2A). Remarkably, BA treatment enhanced remyelination as evaluated by LFB and FluoroMyelin staining (Figure 2B, $p < 0.05$). During 3–6 weeks, CPZ-induced demyelination in the corpus callosum of mice was not altered under BA treatment. However, in 6 + 1 week and 6 + 2 weeks, BA promoted remyelination remarkably compared with the PBS-treated control. As shown in LFB staining test (Figure 2B), BA-treated mice showed a certain recovery of demyelination and a significantly larger remyelination area than that of PBS-treated control at 6 + 1 week and 6 + 2 weeks. In agreement with these findings, the postcuprizone recovery of mature myelin in the body of the corpus callosum of BA-treated group, but not in PBS-treated control, was accelerated by BA supplementation.

Ultrastructural investigations were performed for the quantitative analysis of myelinated axons and confirmed the beneficial effects of BA on remyelination. We found that PBS-treated control exhibited more axons, which were not encased by myelin compared with BA-treated group, and BA treatment increased the number of myelinated axons significantly (Figure 2C). Compared with the highly compact and tightly wrapped myelin in the naïve chow (NC) mice, the newly formed myelin was less tightly wrapped. Consistent with the immunohistochemistry results, thicker myelin sheath was observed in the BA-treated group than that of the PBS-treated control at the 6 + 2 weeks (red arrows). In addition, BA-treated group showed lower *g*-ratios of the myelinated axons compared with the PBS-treated control, indicating a better recovery from demyelination (Figure 2D, $p < 0.01$). These findings suggested that BA treatment enhanced the remyelination in CPZ-induced demyelination model.

Effects of BA on CNS Glial Cells in CPZ-Induced Demyelination Model

To dissect the action of mechanisms of BA in CPZ-induced demyelination model, brain from BA- or PBS-treated group were subjected to histopathologic analyses. Different stages in the OLG maturation cascade, identified by their phenotypic expression of specific markers, were examined in the corpus callosum cross sections by using specific markers of OLG, Olig2, and APC (Figure 3A). An increased number of $Olig2^+$ cells in corpus callosum of the BA-treated group was observed at CPZ-induced 6 + 1 week, in comparison to the PBS-treated group. Double labeling for Olig2+ and APC+ cell was considered as the mature myelinating OLG. Compared with the PBS-treated control, the number of $Olig2^+$ APC^+ cells was increased significantly (~2-fold) in the BA-treated group ($p < 0.05$), which is almost comparable with the NC group ($p > 0.05$), indicating the induction of mature OLG by BA administration.

In addition, immunohistochemical staining revealed a strong increase of the number of GFAP-positive cells in mice exposed to cuprizone, indicating the activation of astrocytes in this model. Significant differences were observed in BA-treated group compared with PBS-treated control. $GFAP^+$ expression increased at CPZ-induced 6 + 2 weeks, with stronger reactivity in BA-treated group (Figure 3B, $p < 0.01$) than that of PBS-treated control. Collectively, these data indicated that BA treatment promoted the differentiation and maturation of OPCs and also reduced the activation of astrocytes.

It is reported that approximately 80% of patients with MS have disturbances in motor functions, such as difficulties in

Figure 2 BA Enhances Remyelination in CPZ-Induced Demyelination Model

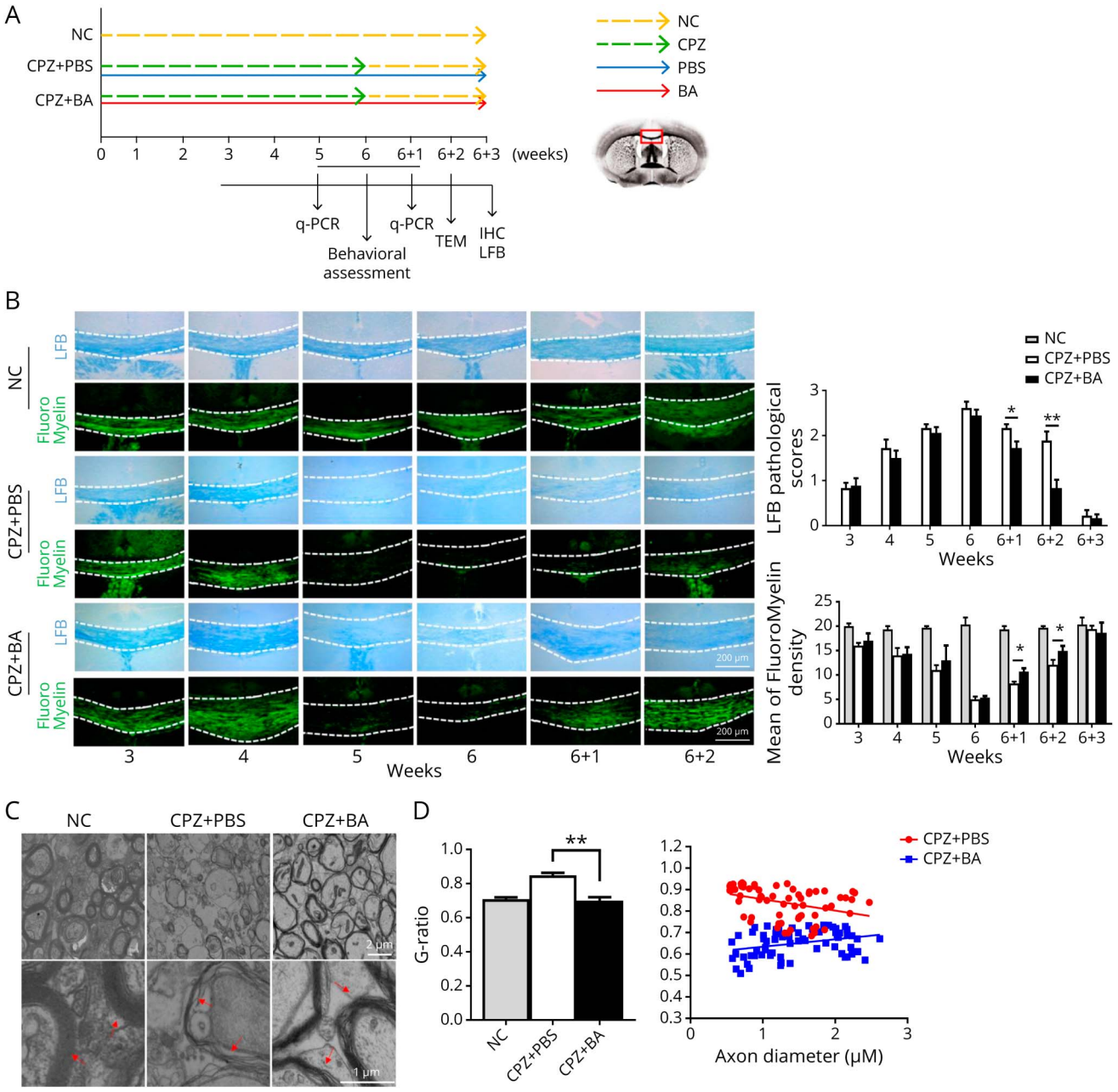

(A) A schematic drawing of demyelination/remyelination mice model. Male, 8- to 10-wk-old C57BL/6 mice were fed with cuprizone for 6 weeks to achieve complete demyelination, followed by feeding normal chow in another 2 weeks. Mice were randomly divided into normal chow + PBS groups (NC, n = 6 and PBS-treated groups (CPZ + PBS, *n* = 12) and BA-treated (CPZ + BA, n = 12), all groups receive BA or PBS treatment starting at CPZ model beginning until the 6 + 3 weeks. A schematic diagram of corpus callosum lateral to lateral ventricle and location observed by paraffin section staining (LFB). (B) LFB and FluoroMyelin staining at different time point (Scale bar, 200 μm). Slices were assessed and scored in a blinded fashion for demyelination: 3, large (confluent); 2, a few areas of demyelination; 1, rare foci; 0, none. The quantification of the mean density of FluoroMyelin staining was performed using ImageJ. (C) Representative electron micrographs at 6 + 2 weeks (Scale bar, 2 μm for the upper row, and 1 μm for the insets in the lower row, rad arrows indicate typical myelin structure in each group). (D) The quantification of myelin G-ratio value (axon diameter/fiber diameter) of NC, CPZ + PBS, and CPZ + BA group. Scatter plot of G-ratio value. Data are shown as mean values ±SEM (*n* = 6 each group). **p* < 0.05, ***p* < 0.01, and ****p* < 0.001 compared with control group, one-way analysis of variance with Tukey multiple comparisons test. BA = baicalin; NC = naïve chow; PBS = phosphate-buffered saline.

maintaining balance, reduced walking speed, and impaired dexterity of the hands and feet.[14] To find out whether the enhanced remyelination in CPZ-induced demyelination by BA resulted in any advantage in sensorimotor function, we performed a behavioral assessment of mice treated with BA or PBS at CPZ-induced 5, 6, and 6 + 1 week (Figure 3C). Sensorimotor and coordination ability was assessed by investigators blinded to group assignments. Mice were initially examined in a beam walking test to evaluate the balance ability. Twenty-four hours later, their muscle coordination was tested by wire hang assay, and the motor coordination was assessed by rotating rod test. In the beam walking test and

Figure 3 Effect of BA Treatment on Astrocyte, Microglia, and Oligodendrocyte Precursor Cell Differentiation in CPZ-Induced Demyelination Model

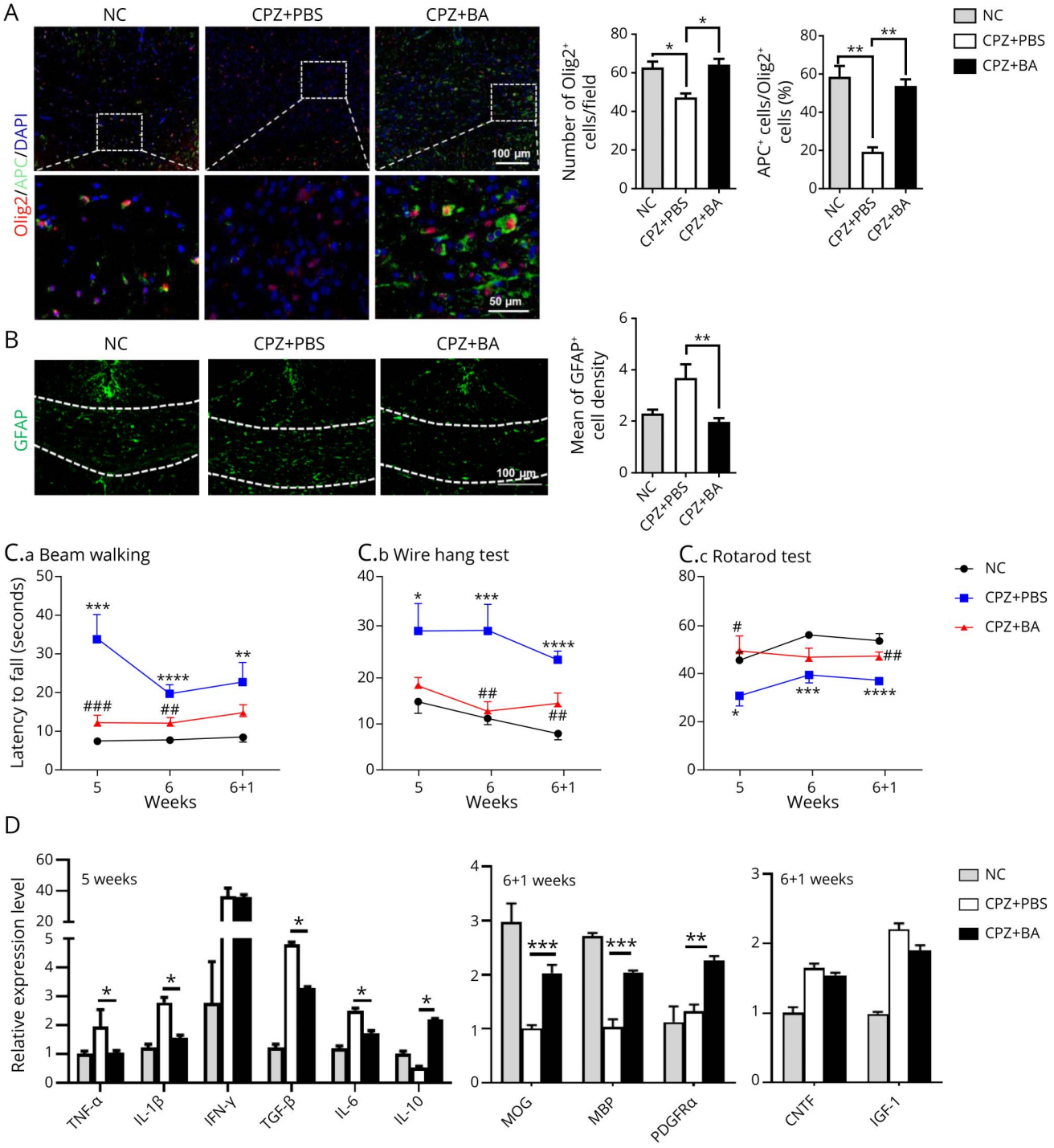

CPZ mice were treated with BA or PBS as shown in Figure 2A. (A) Double immunostaining of Olig2 (red) and APC (green). Scale bar, 100 μm for the upper row, and 50 μm for the insets in the lower row. The quantification of Olig2 positive cells and quantification analysis of the percentage of APC positive cells and Olig2 positive cells measured at random areas using Image-Pro. Date are mean ± SEM (n = 3 each group). (B) GFAP (green) immunostaining at corpus callosum section of all group mice at 6 + 2 weeks (Scale bar, 100 μm). The mean of GFAP-positive cell density was measured in corpus callosum using ImageJ. Data are mean ± SEM (n = 3 each group). (C.a-c) Behavioral assessment (beam walking test (C.a), wire hang test (C.b), and rotating rod test (C.c) of CPZ-induced demyelination mice. (D) The expression of cytokine genes was determined using real-time RT-PCR analysis at CPZ-induced 5 weeks. The expression of myelin-associated protein genes and neurotrophic factors was determined using real-time RT-PCR analysis at CPZ-induced 6 + 1 week. Data are shown as mean values ±SEM (n = 6 each group). *$p < 0.05$, **$p < 0.01$, and ***$p < 0.001$ compared with the control group, one-way analysis of variance with Tukey multiple comparisons test. BA = baicalin; CPZ = cuprizone.

wire hang test, the BA-treated mice used significantly fewer time compared with their PBS-treated control mice, whereas relatively longer time than that of the NC group (Figure 3C). In the rotating rod assay, the BA-treated mice made significantly increased duration of time compared with the PBS-treated control mice (Figure 3C). The behavioral assessment data demonstrated that BA treatment improved long-term sensorimotor and benefitted to the movement coordination and balance of the CPZ-induced demyelination mice.

Given the positive effects of BA on the CNS (re)myelination and neuroinflammation, gene expression of inflammatory and myelin-associated factors in different groups was detected at demyelination stage (5 weeks) and remyelination stage (6 + 1 week), respectively. As shown in Figure 3D, the expression of inflammatory cytokines, including tumor necrosis factor α, IL-1β, interferon γ, transforming growth factor β, and IL-6, was substantially reduced in mice treated with BA at CPZ-induced 5 weeks ($p < 0.05$). BA treatment also increased the production of IL-10, a cytokine that plays roles in anti-inflammatory. Meanwhile, the expression of myelin-associated genes, such as myelin oligodendrocyte glycoprotein, MBP, and PDGFRα, was increased significantly under BA treatment at CPZ-induced 6 + 1 week ($p < 0.05$). The expression of neurotrophic factors, ciliary neurotrophic factor, and insulin-like growth factor 1 were not significantly changed, indicating that the therapeutic effects of BA may not be achieved by these 2 types of neurotrophic factors. Altogether, these results suggested that BA administration improved the CNS inflammatory microenvironment and promoted remyelination effectively.

BA Directly Induced OPC Maturation via PPARγ Signaling

Although our data indicated that BA promoted OLGs differentiation and enhanced remyelination in CPZ-induced demyelination model, there is still a lack of in-depth studies on its target and mechanism of action. Thus, we obtained the molecular docking map of BA into the PPARγ active pocket, which showed that BA could form hydrogen bond interactions with the protein structure of PPARγ at multiple positions (Figure 4A). Subsequently, we performed MST affinity assay experiments, and the results showed that the dissociation constant of BA and PPARγ was 1.35 μM, indicating that the 2 moleculars had affinity cooperation, which was consistent with the results of molecular docking (Figure 4B).

Luciferase activity was further measured by transfecting PPRE×3-TK-luciferase vector in mPPARγ-overexpressing HEK293T cells, followed by stimulation with BA at 10 μg/mL. The results demonstrated that BA treatment could activate PPARγ directly, thus induced the downstream gene (luciferase) expression (Figure 4C, $p < 0.05$).

To verify the function of BA on OPC maturation, we analyzed the effects of BA on primary OPC cultures. Under differentiation conditions, BA treatment (1–10 μg/mL) enhanced OPC maturation into mature OLGs, with myelin-like sheaths and extension of processes, in a dose-dependent manner (Figure 4D, $p < 0.05$). We next investigated the role of PPARγ in BA-mediated myelin gene expression and maturation of primary OPC cultures. Immunofluorescence analysis showed a significant increase in the numbers of MBP positive OLGs and morphological changes. However, this effect was abrogated by GW9662, a PPARγ-specific antagonist. Immunostaining demonstrated that GW9662 blocked BA-induced expression of mature OLG markers (MBP), suggesting that PPARγ activation is essential for the OPC differentiation induced by BA (Figure 4D, $p < 0.01$).

Together, our results indicate that BA acts as a potent promyelinating compound, directly inducing OPC differentiation/maturation relies on the activation of PPARγ activity in OPCs.

Therapeutic Effects of BA on Remyelination Is PPARγ-Dependent in CPZ-Induced Demyelination Model

To further assess that the relationship of BA and PPARγ in vivo, we applied PPARγ$^{\pm}$ to establish the CPZ-induced demyelination model because PPARγ knockout mice is embryonically lethal. After 3 weeks of cuprizone treatment, no significant differences of demyelination was observed between the BA-treated group and PBS-treated and NC group by LFB staining (Figures 5, A and B, $p < 0.05$), suggesting that CPZ-induced demyelination were not inhibited under BA treatment. Remarkably, CPZ-induced PPARγ$^{\pm}$ mice showed stronger demyelination than that of wildtype control. At 6 + 1 week, remyelination effects of BA were also inhibited in PPARγ$^{\pm}$ mice. Immunohistochemical staining revealed a robust increase in the number of GFAP^{+} cells in PPARγ$^{\pm}$ mice exposed to cuprizone compared with wildtype mice, indicating the function of PPARγ in astrocyte activation (Figure 5, C and D, $p < 0.05$ *and* $p > 0.05$). However, there was no significantly a difference in the numbers of IBA1^{+} microglia between the PPARγ$^{\pm}$ and the wildtype mice. Altogether, our results verified that PPARγ play an indispensable role in BA-mediated remyelination.

Discussion

Natural products derived from medicinal plants have long been considered as a rich source of the lead compounds in drug discovery. The irreplaceable advantage of natural compounds, compared with chemical drugs, is their structural complexity and functional diversity. FTY720, the first oral drug for the treatment of relapsing-remitting MS, was isolated from *Cordyceps sinensis* and obtained by structural modification. It is reported that FTY720 not only acts on inhibiting the infiltration of peripheral inflammatory cells into nerve centers[15,16] but also promotes remyelination by inducing the differentiation of OPCs into OLGs in a lysolecithin-induced demyelination model.[15,17] These results confirmed the characteristic of small molecule drugs in multitargets and multieffects.

Figure 4 BA Directly Induced OPC Differentiation via PPARγ Signaling

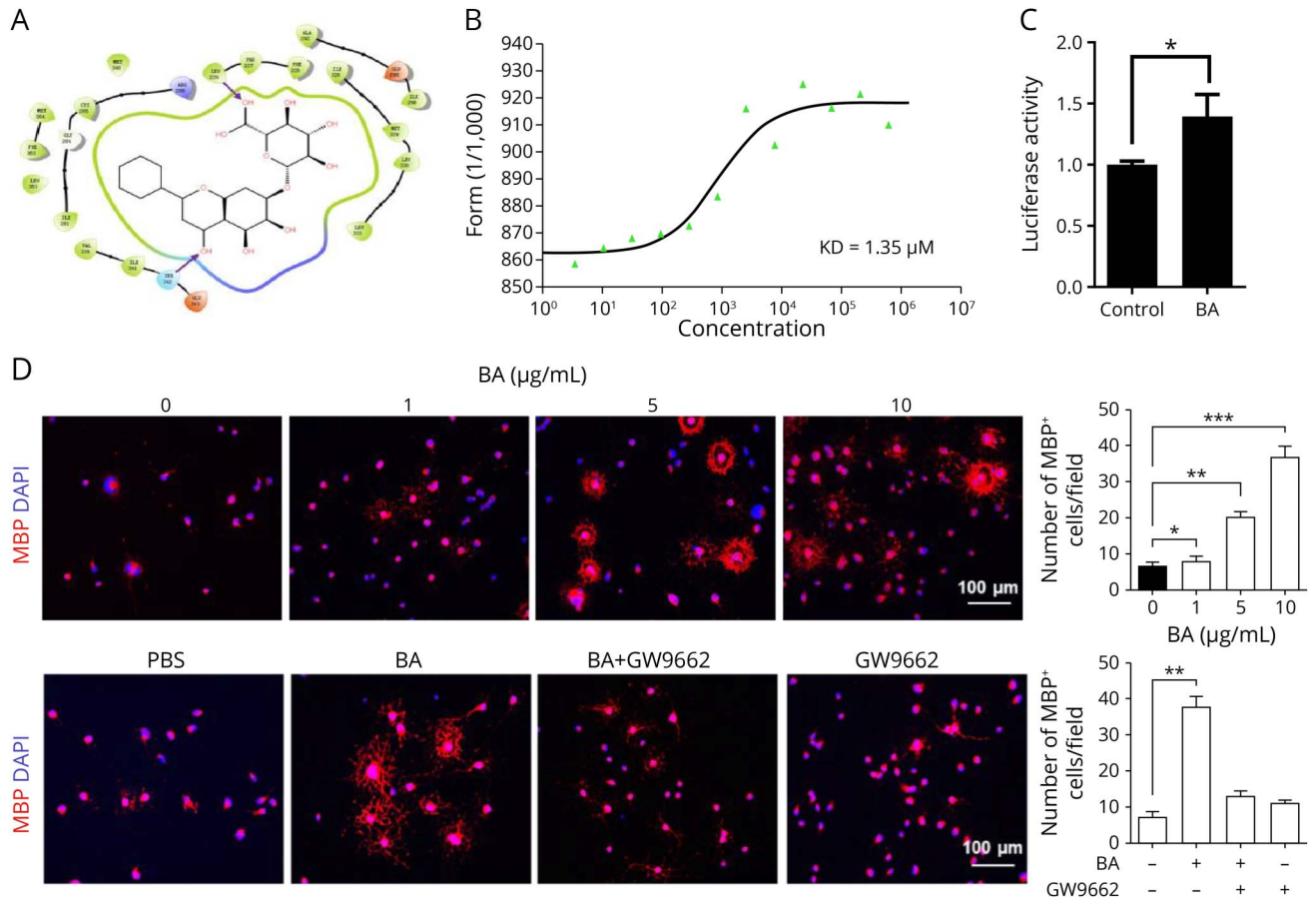

(A) Three-dimensional structure diagram of PPARγ docked with BA. (B) MST affinity determination of BA and PPARγ. (C) HEK293T cells were transfected with PPRE×3-TK-luciferase vector, a PPRE-dependent luciferase reporter constructs. After 24 hours of transfection, cells were cultured with BA of 10 μg/mL for 6 hours, and the activity of luciferase was monitored in cell lysates by a ONE-Glo EX Luciferase Assay System kit (Promega). (D) BA enhanced oligodendrocyte differentiation in primary OPC cultures. Primary OPCs, prepared from brains of newborn C57BL/6 mice, were cultured in the differentiation medium with or without BA (1, 5, or 10 μg/mL) for 5 days, followed by MBP immunofluorescence staining. Primary OPCs were cultured in a differentiation medium with BA (10 μg/mL) alone or pretreated for 30 minutes with GW-9662 (PPARγ-specific antagonist) before addition of BA or GW-9662 (10 nM) alone for 5 days, followed by MBP immunofluorescence staining. Nuclei were stained with DAPI (blue). Scale bar, 50 μm. A quantitative analysis was performed for numbers of MBP^+ mature oligodendrocytes. Data are shown as mean values ± SEM and analyzed by two-tailed Student *t*-test (n = 5 each group). $*p < 0.05$, $**p < 0.01$, and $***p < 0.001$ compared with the control group. BA = baicalin; MBP = myelin basic protein; OPC = oligodendrocyte precursor cell; PPARγ = peroxisome proliferator-activated receptor γ; PPRE = peroxisome proliferator element.

Scutellaria baicalensis, of which BA is the major active compound, has been used for the treatment of a variety of acute and chronic hepatitis and inflammatory disease. BA has been shown to improve memory impairment in Alzheimer disease models[18,19] and promote the proliferation and differentiation of rat neural stem cells.[20] Our previous study demonstrated that BA effectively ameliorates the severity of clinical disease of EAE, an animal model of MS.[10] In this study, we demonstrated that BA-induced OPC differentiation i*n vitro* and promoted CNS remyelination, alleviated astrocyte activation, reduced inflammatory cytokine production, and improved motor dysfunction at effective doses in a noninflammatory demyelination model through the PPARγ signaling pathway. Given that chronic inflammation and white matter damage in the CNS are 2 hallmarks of demyelination diseases, an ideal therapeutic drug has both anti-inflammatory and myelin repair capacities and would be highly beneficial. As a bioactive flavone that is isolated from *S. baicalensis* and officially listed in the Chinese Pharmacopoeia, BA has low toxicity and is well tolerated when administered orally in both humans and rodents.[21,22] In this study, BA dose (100 mg/kg/d) that proved effective for demyelinating disease treatment is approx. 59 times lower than that of its reported acute toxicity (LD50 = 6 g/kg/d).[23] Of note, pharmacokinetic study had clearly demonstrated that the administration of BA could cross the blood–brain barrier and is detectable in the cortex, hippocampus, and striatum,[24] indicating its function in the CNS disorders.

Although the two-pronged beneficial effects of BA are encouraging, it is still unclear whether the myelin-promoting effects of BA is the secondary consequence of the anti-inflammatory activity in the CNS lesion. An important question that the direct effects of BA on myelinogenesis and

Figure 5 Therapeutic Effects of BA on Demyelination Is Peroxisome Proliferator-Activated Receptor γ-Dependent

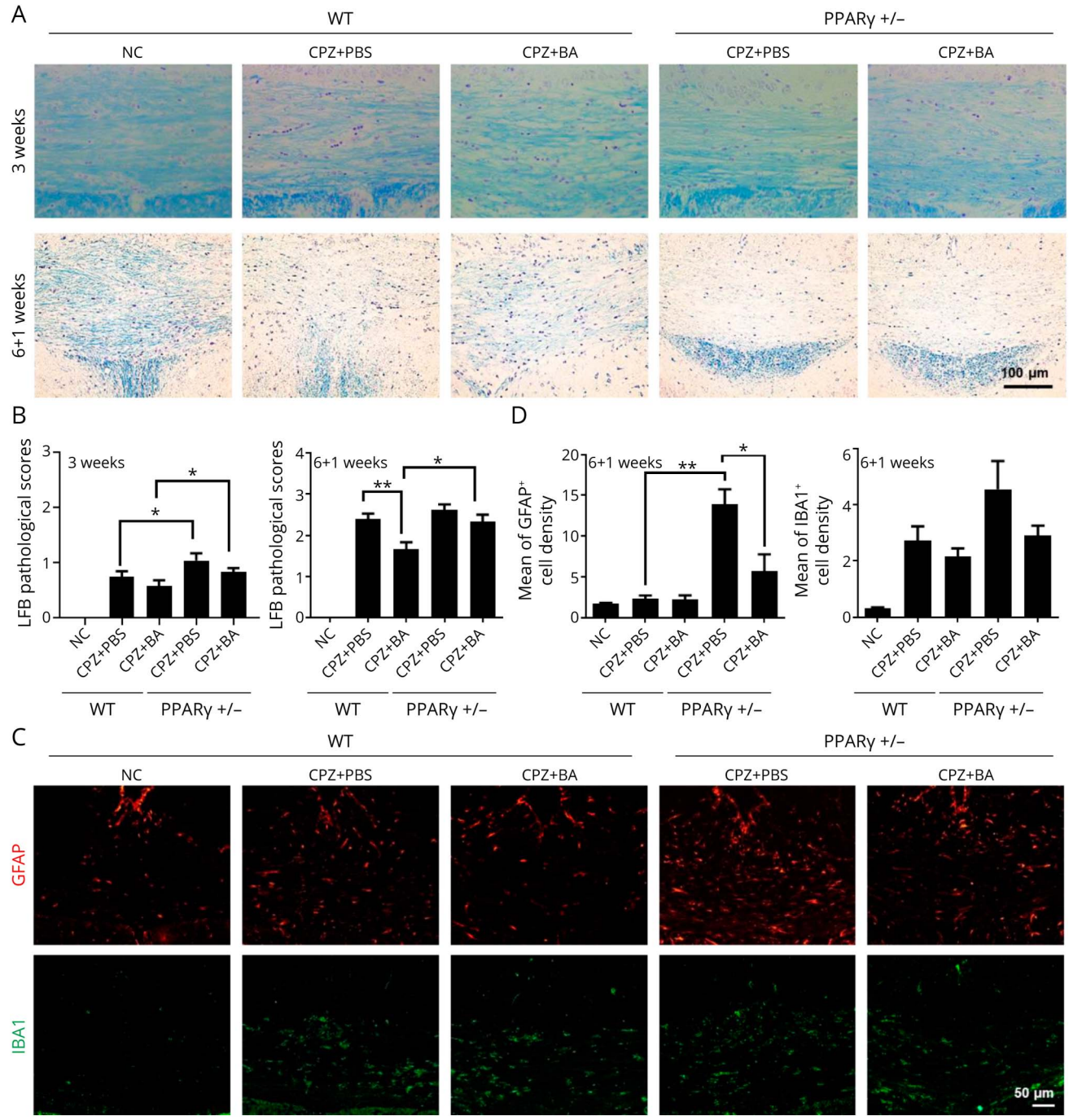

CPZ mice were treated with BA or PBS as shown in Figure 3A. (A) Representative of Luxol fast blue stain. Scale bar, 100 μm. (B) Pathology score of demyelination at 3 weeks and 6 + 1 week (C) GFAP (green) and IBA1 (red) immunostaining at corpus callosum section of all group mice at 6 + 1 week. Scale bar, 50 μm. (D) The mean of GFAP or IBA1 positive cells density was measured in corpus callosum using ImageJ. Data are mean ± SEM (n = 3 each group). *$p < 0.05$, **$p < 0.01$, and ***$p < 0.001$ compared with the control group, one-way analysis of variance with Tukey multiple comparisons test. BA = baicalin; GFAP = glial fibrillary acidic protein; PBS = phosphate-buffered saline.

remyelination under nonpathological conditions or with minimal immune responses should be addressed.[25] In this study, the potential of BA as promyelinating and neurorestorative therapy in nonpathological conditions is clearly highlighted by several lines of evidence. First, when neonatal mice treated with BA at 3 days, 14 days after birth, the development stage of myelinogenesis, BA not only enhanced the numbers of OLG lineage cells in the white matter area of the spinal cord and brain but also increased the number of NFH-labeled extra-axonal MBP and improved the myelin sheath wrapping ability. Second, BA treatment enhanced remyelination and process extension of OLGs after the CPZ-induced demyelination, confirming that BA exert direct promyelination/remyelination effects, which is indispensable for the regeneration

of already damaged CNS tissues. Third, BA treatment drives primary OPCs to mature into OLGs in a dose-dependent manner in vitro. The above results provide a solid foundation to consider BA as a novel therapeutic agent for promoting myelin regeneration.

When OLG differentiation or remyelination is blocked, severe pathologic phenomena are generated. For example, *Shiverer* mice absent myelin sheaths are susceptible to tumors, epilepsy, and ataxia.[26] In human beings, leukodystrophy is a genetic disorder characterized by myelination disorders in the fetus or early infancy,[27,28] with manifestations of intellectual, language, and motor disorders clinically.[29] Myelinogenesis occurs predominantly postnatally (within the first 3 weeks for rodent and 2 years for human, respectively),[30,31] which is an ideal stage to study the promoting effects of drugs on the differentiation and myelination of OPCs under physiologic conditions.[32] It has been proved that the treatment of glatiramer acetate, an approved MS drug, accelerates myelin development in nonpathological condition,[32] demonstrating that the CNS myelination of newborn mice is a valid model for studying myelin development under nonpathological condition. We also confirmed the effect of BA on the developmental process, namely, its ability to promote postnatal myelinogenesis in healthy new-born mice in the physiologic conditions.

Remyelination is the restoration process in which myelin sheaths are wrapped from around the axons to maintain the function of normal conduction.[30] Nevertheless, in the chronic stage of MS, the efficiency of remyelination declines.[33] Therefore, promoting differentiation and myelination of OPCs is essential for the recovery of neurologic function in the patient. To test the direct remyelination effects of BA, we used the CPZ-induced toxic demyelination models with minimal inflammatory and immune-dependent components.[34] The rationale for CPZ-induced toxic demyelination is to produce brain edema, spongiform encephalopathy characterized by massive vacuolar enlargement (intracellular and intramyelinating), and produce morphological images similar to scrapie by administering 0.2%–0.5% (w/w) CPZ to mice in standard rodent chow.[35] In this model, different drug administration times reflect various effects. The dosing cycle through the demyelination and remyelination processes reflects the capacities of drug for inhibiting demyelination and promoting remyelination. Hashimoto et al.[36] reported that mice with BA intraperitoneal injection once-daily for the last 2 weeks (4–6 weeks) of cuprizone exposure can attenuate CPZ-induced demyelination. Compared with these findings, our results reflected that not only the role of BA in demyelination but also the function of BA in promoting remyelination directly.

Furthermore, our study provides detailed evidences of the underlying molecular mechanism and the key signaling events responsible for BA-induced OPCs differentiation and remyelination. Identifying the target of drug action is important for the confirmation of the efficacy of the small molecule drugs.[37] We performed a molecular docking analysis of the possible targets of BA reported in the literature and found that BA could enter the active center of PPARγ. PPARγ, a member of the nuclear receptor superfamily PPAR, is expressed in various cell types, including brain cells such as neurons and glia, and bone marrow-derived immune cells. Substantial evidences indicate that PPARγ is critically involved in the long-term promotion of tissue repair and rescue of brain cells.[38] A recent study demonstrated that PPARγ activation positively contributes to the differentiation of OPCs.[39] However, the mechanism of PPARγ action in the differentiation and function of OPCs in demyelination disease has not yet been described. We found that BA acts on OPC development and remyelination in the CPZ-induced demyelination model and is in a PPARγ-dependent manner because the beneficial effects of BA were blocked remarkably in PPARγ-deficient mice. To our knowledge, this is the first demonstration that BA regulates OPC differentiation and function through the PPARγ pathway. PPARγ ligands can be classified into 3 major categories,[38] including (1) natural (endogenous) agonist-like unsaturated fatty acids, (2) synthetic agonists such as pioglitazone (PGZ), ciglitazone (CGZ),[40] and (3) synthetic antagonist-like bisphenol A diglyceryl ether (GW9662). Our study here provides persuasive evidence that natural compound BA acts as a novel agonist with a good safety record and minimal side effects in clinical.

In general, our findings give an important insight into the myelin repair capacities of BA through promoting OLG maturation and remyelination in different models via the PPARγ signal pathway. These studies, together with well-known anti-inflammation activity of BA, its safety record in clinical, its low cost and easy availability traits, pave the way for clinical applications in the demyelination diseases, for which there is currently no effective therapy.

Study Funding

This study was supported by the Chinese National Natural Science Foundation (Grant No. 81771345, 82071396, 31970771), the Natural Science Foundation of Shaanxi Province, China (Grant No. 2019KJXX-022, 2021ZDLSF03-09), the Fundamental Research Funds for the Central Universities (Grant No. GK202105002, GK202007022, 2019TS080, 2020CSLZ010).

Disclosure

The authors report no disclosures relevant to the manuscript. Go to Neurology.org/NN for full disclosures.

Publication History

Received by *Neurology: Neuroimmunology & Neuroinflammation* August 19, 2021. Accepted in final form December 10, 2021.

Appendix Authors

Name	Location	Contribution
Ruo-Song Ai, PhD	Shaanxi Normal University, Xi'an, China	Drafting/revision of the manuscript for content, including medical writing for content, and major role in the acquisition of data

Appendix *(continued)*

Name	Location	Contribution
Kun Xing, MSc	Shaanxi Normal University, Xi'an, China	Drafting/revision of the manuscript for content, including medical writing for content, and major role in the acquisition of data
Xin Deng, MSc	Shaanxi Normal University, Xi'an, China	Drafting/revision of the manuscript for content, including medical writing for content, and major role in the acquisition of data
Juan-Juan Han, MSc	Shaanxi Normal University, Xi'an, China	Drafting/revision of the manuscript for content, including medical writing for content, and major role in the acquisition of data
Dong-Xia Hao, MSc	Shaanxi Normal University, Xi'an, China	Major role in the acquisition of data
Wen-Hui Qi, MSc	Shaanxi Normal University, Xi'an, China	Major role in the acquisition of data
Bing Han, PhD	Shaanxi Normal University, Xi'an, China	Study concept or design
Ya-Na Yang, MSc	Shaanxi Normal University, Xi'an, China	Study concept or design
Xing Li, PhD	Shaanxi Normal University, Xi'an, China	Study concept or design
Yuan Zhang, PhD	Shaanxi Normal University, Xi'an, China	Drafting/revision of the manuscript for content, including medical writing for content, study concept or design, and analysis or interpretation of data

References

1. Goldman SA, Nedergaard M, Windrem MS. Glial progenitor cell-based treatment and modeling of neurological disease. *Science.* 2012;338(6106):491-495
2. Chen JF, Liu K, Hu B, et al. Enhancing myelin renewal reverses cognitive dysfunction in a murine model of Alzheimer's disease. *Neuron.* 2021;109(14):2292-2307.e5.
3. Wang F, Ren SY, Chen JF, et al. Myelin degeneration and diminished myelin renewal contribute to age-related deficits in memory. *Nat Neurosci.* 2020;23(4):481-486.
4. Franklin RJM, Ffrench-Constant C. Remyelination in the CNS: from biology to therapy. *Nat Rev Neurosci.* 2008;9(11):839-855.
5. Kremer D, Göttle P, Hartung HP, Küry P. Pushing forward: remyelination as the new frontier in CNS diseases. *Trends Neurosci.* 2016;39(4):246-263.
6. Li M, Shi A, Pang H, et al. Safety, tolerability, and pharmacokinetics of a single ascending dose of baicalein chewable tablets in healthy subjects. *J Ethnopharmacol.* 2014;156:210-215.
7. Najm FJ, Madhavan M, Zaremba A, et al. Drug-based modulation of endogenous stem cells promotes functional remyelination in vivo. *Nature.* 2015;522(7555):216-220.
8. Li-Weber M. New therapeutic aspects of flavones: the anticancer properties of Scutellaria and its main active constituents Wogonin, Baicalein and Baicalin. *Cancer Treat Rev.* 2009;35(1):57-68.
9. Srinivas NR. Baicalin, an emerging multi-therapeutic agent: pharmacodynamics, pharmacokinetics, and considerations from drug development perspectives. *Xenobiotica.* 2010;40(5):357-367.
10. Zhang Y, Li X, Ciric B, et al. Therapeutic effect of baicalin on experimental autoimmune encephalomyelitis is mediated by SOCS3 regulatory pathway. *Sci Rep.* 2015;5(1):17407.
11. Zhang Y, Li X, Ciric B, et al. A dual effect of ursolic acid to the treatment of multiple sclerosis through both immunomodulation and direct remyelination. *Proc Natl Acad Sci U S A.* 2020;117(16):9082-9093.
12. Skripuletz T, Miller E, Moharregh-Khiabani D, et al. Beneficial effects of minocycline on cuprizone induced cortical demyelination. *Neurochem Res.* 2010;35(9):1422-1433.
13. Scoles DR, Meera P, Schneider MD, et al. Antisense oligonucleotide therapy for spinocerebellar ataxia type 2. *Nature.* 2017;544(7650):362-366.
14. Benedict RHB, Holtzer R, Motl RW, et al. Upper and lower extremity motor function and cognitive impairment in multiple sclerosis. *J Int Neuropsychol Soc.* 2011;17(4):643-653.
15. Miron VE, Ludwin SK, Darlington PJ, et al. Fingolimod (FTY720) enhances remyelination following demyelination of organotypic cerebellar slices. *Am J Pathol.* 2010;176(6):2682-2694.
16. Brinkmann V, Billich A, Baumruker T, et al. Fingolimod (FTY720): discovery and development of an oral drug to treat multiple sclerosis. *Nat Rev Drug Discov.* 2010;9(11):883-897.
17. Moyon S, Frawley R, Marechal D, et al. TET1-mediated DNA hydroxymethylation regulates adult remyelination in mice. *Nat Commun.* 2021;12(1):3359.
18. Wang HZ, Wang HH, Huang SS, et al. Inhibitory effect of baicalin on collagen-induced arthritis in rats through the nuclear factor– κ B pathway. *J Pharmacol Exp Ther.* 2014;350(2):435-443.
19. Chen C, Li X, Gao P, et al. Baicalin attenuates Alzheimer-like pathological changes and memory deficits induced by amyloid β1–42 protein. *Metab Brain Dis.* 2015;30(2):537-544.
20. Zhao J, Lu S, Yu H, Duan S, Zhao J. Baicalin and ginsenoside Rb1 promote the proliferation and differentiation of neural stem cells in Alzheimer's disease model rats. *Brain Res.* 2018;1678:187-194.
21. Singh S, Meena A, Luqman S. Baicalin mediated regulation of key signaling pathways in cancer. *Pharmacol Res.* 2021;164:105387.
22. Moghaddam E, Teoh BT, Sam SS, et al. Baicalin, a metabolite of baicalein with antiviral activity against dengue virus. *Sci Rep.* 2015;4(1):5452.
23. Dai J, Liang K, Zhao S, et al. Chemoproteomics reveals baicalin activates hepatic CPT1 to ameliorate diet-induced obesity and hepatic steatosis. *Proc Natl Acad Sci.* 2018;115(26):E5896-E5905.
24. Zhang L, Xing D, Wang W, Wang R, Du L. Kinetic difference of baicalin in rat blood and cerebral nuclei after intravenous administration of Scutellariae Radix extract. *J Ethnopharmacol.* 2006;103(1):120-125.
25. Kanakasabai S, Pestereva E, Chearwae W, Gupta SK, Ansari S, Bright JJ. PPARγ agonists promote oligodendrocyte differentiation of neural stem cells by modulating stemness and differentiation genes. *PLoS One.* 2012;7(11):e50500.
26. Duncan ID, Kondo Y, Zhang SC. The myelin mutants as models to study myelin repair in the leukodystrophies. *Neurotherapeutics.* 2011;8(4):607-624.
27. Kohlschütter A, Eichler F. Childhood leukodystrophies: a clinical perspective. *Expert Rev Neurother.* 2011;11(10):1485-1496.
28. Yeung MSY, Djelloul M, Steiner E, et al. Dynamics of oligodendrocyte generation in multiple sclerosis. *Nature.* 2019;566(7745):538-542.
29. Turón-Viñas E, Pineda M, Cusí V, et al. Vanishing white matter disease in a Spanish population. *J Cent Nerv Syst Dis.* 2014;6:59-68.
30. Yeung MSY, Zdunek S, Bergmann O, et al. Dynamics of oligodendrocyte generation and myelination in the human brain. *Cell.* 2014;159(4):766-774.
31. Abiraman K, Pol SU, O'Bara MA, et al. Anti-muscarinic adjunct therapy accelerates functional human oligodendrocyte repair. *J Neurosci.* 2015;35(8):3676-3688.
32. From R, Eilam R, Bar-Lev DD, et al. Oligodendrogenesis and myelinogenesis during postnatal development effect of glatiramer acetate: GA Promotes Oligogenesis and Myelinogenesis. *Glia* 2014;62(4):649-665.
33. Franklin RJM. Regenerative medicines for remyelination: from aspiration to reality. *Cell Stem Cell* 2015;16(6):576-577.
34. Praet J, Guglielmetti C, Berneman Z, Van der Linden A, Ponsaerts P. Cellular and molecular neuropathology of the cuprizone mouse model: clinical relevance for multiple sclerosis. *Neurosci Biobehav Rev.* 2014;47:485-505.
35. Scott-Hewitt NJ, Folts CJ, Hogestyn JM, Piester G, Mayer-Pröschel M, Noble MD. Heterozygote galactocerebrosidase (GALC) mutants have reduced remyelination and impaired myelin debris clearance following demyelinating injury. *Hum Mol Genet.* 2017;26(15):2825-2837.
36. Hashimoto M, Yamamoto S, Iwasa K, et al. The flavonoid Baicalein attenuates cuprizone-induced demyelination via suppression of neuroinflammation. *Brain Res Bull.* 2017;135:47-52.
37. Yue R, Shan L, Yang X, Zhang W. Approaches to target profiling of natural products. *Curr Med Chem.* 2012;19(22):3841-3855.
38. Cai W, Yang T, Liu H, et al. Peroxisome proliferator-activated receptor γ (PPARγ): a master gatekeeper in CNS injury and repair. *Prog Neurobiol.* 2018;163-164:27-58.
39. Pu H, Zheng X, Jiang X, et al. Interleukin-4 improves white matter integrity and functional recovery after murine traumatic brain injury via oligodendroglial PPARγ. *J Cereb Blood Flow Metab.* 2021;41(3):511-529.
40. Li X, Du J, Xu S, Lin X, Ling Z. Peroxisome proliferator-activated receptor-γ agonist rosiglitazone reduces secondary damage in experimental spinal cord injury. *J Int Med Res.* 2013;41(1):153-161.